

AXIALVECTOR TETRAQUARK CANDIDATES FOR THE $Z_c(3900)$, $Z_c(4020)$, $Z_c(4430)$, $Z_c(4600)$

Zhi-Gang Wang ¹

Department of Physics, North China Electric Power University, Baoding 071003, P. R. China

Abstract

In this paper, we construct the axialvector and tensor current operators to investigate the ground state tetraquark states and the first radially excited tetraquark states with the quantum numbers $J^{PC} = 1^{+-}$ via the QCD sum rules systematically, and observe that there are one axialvector tetraquark candidate for the $Z_c(3900)$ and $Z_c(4430)$, two axialvector tetraquark candidates for the $Z_c(4020)$, three axialvector tetraquark candidates for the $Z_c(4600)$.

PACS number: 12.39.Mk, 12.38.Lg

Key words: Tetraquark state, QCD sum rules

1 Introduction

In 2019, the LHCb collaboration performed an angular analysis of the weak decays $B^0 \rightarrow J/\psi K^+ \pi^-$ using proton-proton collision data, examined the $m(J/\psi \pi^-)$ versus the $m(K^+ \pi^-)$ plane, and observed two possible resonant structures in the vicinity of the energies $m(J/\psi \pi^-) = 4200$ MeV and 4600 MeV, respectively [1]. There have been two tentative assignments of the structure $Z_c(4600)$ in the vicinity of $m(J/\psi \pi^-) = 4600$ MeV, the $[dc]_P[\bar{u}\bar{c}]_A - [dc]_A[\bar{u}\bar{c}]_P$ type vector tetraquark state with $J^{PC} = 1^{--}$ [2] and the first radially excited $[dc]_T[\bar{u}\bar{c}]_A - [dc]_A[\bar{u}\bar{c}]_T$ type tetraquark state with $J^{PC} = 1^{+-}$ [3]. In this paper, we use the subscripts P , S , V , A and T to represent the pseudoscalar, scalar, vector, axialvector and tensor color-antitriplet diquark states, respectively.

In 2013, the BESIII collaboration observed the charged charmonium-like resonance $Z_c^\pm(3900)$ in the $\pi^\pm J/\psi$ invariant mass spectrum in the process $e^+e^- \rightarrow J/\psi \pi^+ \pi^-$ with $M_{Z_c} = (3899.0 \pm 3.6 \pm 4.9)$ MeV and $\Gamma_{Z_c} = (46 \pm 10 \pm 20)$ MeV, respectively [4]. The Belle collaboration also observed the $Z_c^\pm(3900)$ in the same process [5], furthermore, the CLEO collaboration confirmed the existence of the $Z_c^\pm(3900)$ [6]. Almost at the same time, the BESIII collaboration observed the charmonium-like resonance $Z_c^\pm(4025)$ in the vicinity of the threshold $(D^* \bar{D}^*)^\pm$ in the electron-positron scattering process $e^+e^- \rightarrow (D^* \bar{D}^*)^\pm \pi^\mp$ [7]. Moreover, the BESIII collaboration observed the charmonium-like resonance $Z_c^\pm(4020)$ in the $\pi^\pm h_c$ invariant mass spectrum in the electron-positron collisions $e^+e^- \rightarrow \pi^+ \pi^- h_c$ [8]. Now the $Z_c^\pm(4020)$ and $Z_c^\pm(4025)$ are listed in *The Review of Particle Physics* as the same particle [9]. In 2014, the LHCb collaboration performed a four-dimensional fit of the scattering amplitude for the decay $B^0 \rightarrow \psi' \pi^- K^+$ in proton-proton collisions, and obtained the first independent confirmation of the charmonium-like resonance $Z_c^-(4430)$ and determined its quantum numbers to be $J^P = 1^+$ [10]. In 2017, the BESIII collaboration established the charmonium-like resonance $Z_c(3900)$'s quantum numbers to be $J^P = 1^+$ [11].

There have been several possible explanations for the exotic states $Z_c(3900)$ and $Z_c(4020)$, such as the molecular states (from the heavy quark symmetries [12, 13], the QCD sum rules [14, 15], the light-front quark model [16], the one-pion exchange model [17], and the phenomenological Lagrangian approach [18]), the tetraquark states (from the diquark model with the effective Hamiltonian [19], the QCD sum rules [20, 21, 22, 23], and the potential model [24]), the triangle singularities (in the rescattering amplitudes) [25], the threshold effects [26], etc.

We can tentatively assign the hidden-charm resonances $Z_c(3900)$ and $Z_c(4430)$ as the ground state tetraquark state and the first radially excited tetraquark state respectively considering the similar decays, $Z_c(3900)^\pm \rightarrow J/\psi \pi^\pm$, $Z_c(4430)^\pm \rightarrow \psi' \pi^\pm$, and the almost equal energy gaps $M_{Z_c(4430)} - M_{Z_c(3900)} = 591$ MeV, $M_{\psi'} - M_{J/\psi} = 589$ MeV [27, 28]. In Ref.[29], we adopt the method invented in Ref.[30] for the conventional quarkonium to study the $Z_c^\pm(3900)$ as the

¹E-mail: zgwang@aliyun.com.

ground state axialvector tetraquark state and the $Z_c^\pm(4430)$ as the first radially excited axialvector tetraquark state respectively, and employ the energy scale formula $\mu = \sqrt{M_{X/Y/Z}^2 - (2\mathbb{M}_c)^2}$ to select the best energy scales of the spectral densities at the QCD side of the QCD sum rules with the effective (or constituent) charm quark mass \mathbb{M}_c [31]. In Ref.[32], this subject is studied with the QCD sum rules adopting another parameter system. In Refs.[22, 23], we observe that we can assign the $Z_c(4020/4025)$ to be the ground state axialvector $[uc]_A[\bar{d}\bar{c}]_A$ tetraquark state with the quantum numbers $J^{PC} = 1^{+-}$ according to the QCD sum rules calculations. If the $Z_c(4600)$ is the first radial excitation of the hidden-charm tetraquark candidate $Z_c(4020/4025)$, its preferred decay mode is $Z_c(4600) \rightarrow \psi'\pi$ rather than $Z_c(4600) \rightarrow J/\psi\pi$.

In this paper, we intend to perform a detailed and updated analysis of the ground states and the first radially excited states of the charged hidden-charm tetraquark states with the QCD sum rules, and explore the possible assignments of the $Z_c(4600)$ state in the scenario of the axialvector hidden-charm tetraquark states with the quantum numbers $J^{PC} = 1^{+-}$.

The paper is arranged as follows: in Sect.2 we obtain the analytical expressions of the QCD sum rules for the hidden-charm axialvector tetraquark states Z_c ; in Sect.3 we provide the numerical results for the masses and pole residues of the Z_c states and detailed discussions; in Sect.4 we reach the conclusion.

2 The QCD sum rules for the axialvector tetraquark states

In the following, let us write down the two-point Green functions (or correlation functions) $\Pi_{\mu\nu}(p)$ and $\Pi_{\mu\nu\alpha\beta}(p)$ as the first step,

$$\begin{aligned}\Pi_{\mu\nu}(p) &= i \int d^4x e^{ip \cdot x} \langle 0 | T \{ J_\mu(x) J_\nu^\dagger(0) \} | 0 \rangle, \\ \Pi_{\mu\nu\alpha\beta}(p) &= i \int d^4x e^{ip \cdot x} \langle 0 | T \{ J_{\mu\nu}(x) J_{\alpha\beta}^\dagger(0) \} | 0 \rangle,\end{aligned}\quad (1)$$

where the four-quark current operators $J_\mu(x) = J_\mu^1(x), J_\mu^2(x), J_\mu^3(x)$,

$$\begin{aligned}J_\mu^1(x) &= \frac{\varepsilon^{ijk}\varepsilon^{imn}}{\sqrt{2}} \left[u^{Tj}(x) C \gamma_5 c^k(x) \bar{d}^m(x) \gamma_\mu C \bar{c}^{Tn}(x) - u^{Tj}(x) C \gamma_\mu c^k(x) \bar{d}^m(x) \gamma_5 C \bar{c}^{Tn}(x) \right], \\ J_\mu^2(x) &= \frac{\varepsilon^{ijk}\varepsilon^{imn}}{\sqrt{2}} \left[u^{Tj}(x) C \sigma_{\mu\nu} \gamma_5 c^k(x) \bar{d}^m(x) \gamma^\nu C \bar{c}^{Tn}(x) - u^{Tj}(x) C \gamma^\nu c^k(x) \bar{d}^m(x) \gamma_5 \sigma_{\mu\nu} C \bar{c}^{Tn}(x) \right], \\ J_\mu^3(x) &= \frac{\varepsilon^{ijk}\varepsilon^{imn}}{\sqrt{2}} \left[u^{Tj}(x) C \sigma_{\mu\nu} c^k(x) \bar{d}^m(x) \gamma_5 \gamma^\nu C \bar{c}^{Tn}(x) + u^{Tj}(x) C \gamma^\nu \gamma_5 c^k(x) \bar{d}^m(x) \sigma_{\mu\nu} C \bar{c}^{Tn}(x) \right], \\ J_{\mu\nu}(x) &= \frac{\varepsilon^{ijk}\varepsilon^{imn}}{\sqrt{2}} \left[u^{Tj}(x) C \gamma_\mu c^k(x) \bar{d}^m(x) \gamma_\nu C \bar{c}^{Tn}(x) - u^{Tj}(x) C \gamma_\nu c^k(x) \bar{d}^m(x) \gamma_\mu C \bar{c}^{Tn}(x) \right],\end{aligned}\quad (2)$$

the superscripts i, j, k, m and n are color indexes with values obeying the antisymmetric tensor ε , the charge conjugation matrix $C = i\gamma^2\gamma^0$. If we perform charge conjugation (and parity) transform \widehat{C} (and \widehat{P}), the axialvector current operators $J_\mu(x)$ and tensor current operator $J_{\mu\nu}(x)$ have the following properties,

$$\begin{aligned}\widehat{C} J_\mu(x) \widehat{C}^{-1} &= -J_\mu(x), \\ \widehat{C} J_{\mu\nu}(x) \widehat{C}^{-1} &= -J_{\mu\nu}(x), \\ \widehat{P} J_\mu(x) \widehat{P}^{-1} &= -J^\mu(\tilde{x}), \\ \widehat{P} J_{\mu\nu}(x) \widehat{P}^{-1} &= J^{\mu\nu}(\tilde{x}),\end{aligned}\quad (3)$$

where the coordinates $x^\mu = (t, \vec{x})$ and $\tilde{x}^\mu = (t, -\vec{x})$.

The diquark operators $\varepsilon^{ijk} q_j^T C \Gamma Q_k$ in the attractive color-antitriplet $\bar{3}_c$ channel have five spinor structures, where $C\Gamma = C\gamma_5$, C , $C\gamma_\mu\gamma_5$, $C\gamma_\mu$ and $C\sigma_{\mu\nu}$ or $C\sigma_{\mu\nu}\gamma_5$ correspond to the scalar, pseudoscalar, vector, axialvector and tensor diquark operators, respectively. The favorable quark-quark correlations are the scalar diquark and axialvector diquark in the color-antitriplet $\bar{3}_c$ channel from the QCD sum rules [33]. If we introduce a relative P-wave between the light quark and heavy quark, we can obtain the pseudoscalar diquark operator $\varepsilon^{ijk} q_j^T C \gamma_5 \underline{\gamma_5} Q_k$ and vector diquark operator $\varepsilon^{ijk} q_j^T C \gamma_\mu \underline{\gamma_5} Q_k$ without introducing the additional P-wave explicitly, as multiplying a γ_5 can change the parity, the P-wave effect is embodied in the underlined γ_5 . The pseudoscalar diquark states and vector diquark states (or the P-wave diquark states) have larger masses compared with the scalar diquark states and axialvector diquark states, we would like to choose the scalar diquark and axialvector diquark to construct the four-quark current operators to interpolate the lower tetraquark states.

The tensor heavy diquark operators $\varepsilon^{abc} q_b^T(x) C \sigma_{\mu\nu} \gamma_5 Q_c(x)$ and $\varepsilon^{abc} q_b^T(x) C \sigma_{\mu\nu} Q_c(x)$ have both axialvector constituents and vector constituents,

$$\begin{aligned}
\hat{P} \varepsilon^{abc} q_b^T(x) C \sigma_{jk} \gamma_5 Q_c(x) \hat{P}^{-1} &= +\varepsilon^{abc} q_b^T(\tilde{x}) C \sigma_{jk} \gamma_5 Q_c(\tilde{x}), \\
\hat{P} \varepsilon^{abc} q_b^T(x) C \sigma_{0j} Q_c(x) \hat{P}^{-1} &= +\varepsilon^{abc} q_b^T(\tilde{x}) C \sigma_{0j} Q_c(\tilde{x}), \\
\hat{P} \varepsilon^{abc} q_b^T(x) C \sigma_{0j} \gamma_5 Q_c(x) \hat{P}^{-1} &= -\varepsilon^{abc} q_b^T(\tilde{x}) C \sigma_{0j} \gamma_5 Q_c(\tilde{x}), \\
\hat{P} \varepsilon^{abc} q_b^T(x) C \sigma_{jk} Q_c(x) \hat{P}^{-1} &= -\varepsilon^{abc} q_b^T(\tilde{x}) C \sigma_{jk} Q_c(\tilde{x}),
\end{aligned} \tag{4}$$

where the space indexes $j, k = 1, 2, 3$. The tensor diquark operators also play an important role in constructing the tetraquark current operators [34]. We multiply the tensor diquark (antidiquark) operators with the axialvector or vector antidiquark (diquark) operators so as to project out the axialvector constituents and vector constituents to construct the four-quark current operators $J_\mu^2(x)$ and $J_\mu^3(x)$. Thereafter, we will use the \tilde{V} and \tilde{A} to represent the vector constituent and axialvector constituent of the tensor diquark operators, respectively.

The four-quark current operators $J_\mu^1(x)$, $J_\mu^2(x)$ and $J_\mu^3(x)$ couple potentially to the $[uc]_S[\bar{d}\bar{c}]_A - [uc]_A[\bar{d}\bar{c}]_S$ type, $[uc]_{\tilde{A}}[\bar{d}\bar{c}]_A - [uc]_A[\bar{d}\bar{c}]_{\tilde{A}}$ type and $[uc]_{\tilde{V}}[\bar{d}\bar{c}]_V + [uc]_V[\bar{d}\bar{c}]_{\tilde{V}}$ type axialvector hidden-charm tetraquark states with the spin-parity-charge-conjugation $J^{PC} = 1^{+-}$, respectively. While the current operator $J_{\mu\nu}(x)$ couples potentially to both the $[uc]_A[\bar{d}\bar{c}]_A$ type axialvector tetraquark state with $J^{PC} = 1^{+-}$ and vector tetraquark state with $J^{PC} = 1^{--}$. Thereafter, we will not distinguish the negative or positive electric-charge of the Z_c tetraquark states, as they have degenerate masses.

We insert a complete set of hadron states which have nonvanishing couplings with the four-quark current operators $J_\mu(x)$ and $J_{\mu\nu}(x)$ into the Green functions $\Pi_{\mu\nu}(p)$ and $\Pi_{\mu\nu\alpha\beta}(p)$ to get the hadronic representation [35, 36]. Then we separate the ground state axialvector and vector tetraquark state contributions from other contributions, such as the higher excited tetraquark states and continuum states, to obtain the results,

$$\begin{aligned}
\Pi_{\mu\nu}(p) &= \frac{\lambda_Z^2}{m_Z^2 - p^2} \left(-g_{\mu\nu} + \frac{p_\mu p_\nu}{p^2} \right) + \dots \\
&= \Pi_Z(p^2) \left(-g_{\mu\nu} + \frac{p_\mu p_\nu}{p^2} \right) + \dots,
\end{aligned} \tag{5}$$

$$\begin{aligned}
\Pi_{\mu\nu\alpha\beta}(p) &= \frac{\tilde{\lambda}_Z^2}{m_Z^2 - p^2} (p^2 g_{\mu\alpha} g_{\nu\beta} - p^2 g_{\mu\beta} g_{\nu\alpha} - g_{\mu\alpha} p_\nu p_\beta - g_{\nu\beta} p_\mu p_\alpha + g_{\mu\beta} p_\nu p_\alpha + g_{\nu\alpha} p_\mu p_\beta) \\
&\quad + \frac{\tilde{\lambda}_Y^2}{m_Y^2 - p^2} (-g_{\mu\alpha} p_\nu p_\beta - g_{\nu\beta} p_\mu p_\alpha + g_{\mu\beta} p_\nu p_\alpha + g_{\nu\alpha} p_\mu p_\beta) + \dots \\
&= \Pi_Z(p^2) (p^2 g_{\mu\alpha} g_{\nu\beta} - p^2 g_{\mu\beta} g_{\nu\alpha} - g_{\mu\alpha} p_\nu p_\beta - g_{\nu\beta} p_\mu p_\alpha + g_{\mu\beta} p_\nu p_\alpha + g_{\nu\alpha} p_\mu p_\beta) \\
&\quad + \Pi_Y(p^2) (-g_{\mu\alpha} p_\nu p_\beta - g_{\nu\beta} p_\mu p_\alpha + g_{\mu\beta} p_\nu p_\alpha + g_{\nu\alpha} p_\mu p_\beta),
\end{aligned} \tag{6}$$

where the Z represents the axialvector tetraquark states, the Y represents the vector tetraquark states, the λ_Z , λ_Y and $\tilde{\lambda}_Y$ are the pole residues or current-tetraquark coupling constants,

$$\begin{aligned}\langle 0|J_\mu(0)|Z_c(p)\rangle &= \lambda_Z \varepsilon_\mu, \\ \langle 0|J_{\mu\nu}(0)|Z_c(p)\rangle &= \tilde{\lambda}_Z \varepsilon_{\mu\nu\alpha\beta} \varepsilon^\alpha p^\beta, \\ \langle 0|J_{\mu\nu}(0)|Y(p)\rangle &= \tilde{\lambda}_Y (\varepsilon_\mu p_\nu - \varepsilon_\nu p_\mu),\end{aligned}\tag{7}$$

the antisymmetric tensor $\varepsilon_{0123} = -1$, the $\varepsilon_\mu(\lambda, p)$ are the polarization vectors of the axialvector and vector tetraquark states satisfy the summation formula,

$$\sum_\lambda \varepsilon_\mu^*(\lambda, p) \varepsilon_\nu(\lambda, p) = -g_{\mu\nu} + \frac{p_\mu p_\nu}{p^2}.\tag{8}$$

The diquark-antidiquark type four-quark current operators $J_\mu(x)$ and $J_{\mu\nu}(x)$ couple potentially to the diquark-antidiquark type hidden-charm tetraquark states. We can perform Fierz rearrangements to those currents in both the spinor space and color space to obtain a series of color-singlet-color-singlet (or meson-meson) type current operators, for example,

$$\begin{aligned}J_\mu^1(x) &= \frac{1}{2\sqrt{2}} \left\{ i\bar{c}(x)i\gamma_5 c(x) \bar{d}(x)\gamma^\mu u(x) - i\bar{c}(x)\gamma^\mu c(x) \bar{d}(x)i\gamma_5 u(x) + \bar{c}(x)u(x) \bar{d}(x)\gamma^\mu \gamma_5 c(x) \right. \\ &\quad - \bar{c}(x)\gamma^\mu \gamma_5 u(x) \bar{d}(x)c(x) - i\bar{c}(x)\gamma_\nu \gamma_5 c(x) \bar{d}(x)\sigma^{\mu\nu} u(x) + i\bar{c}(x)\sigma^{\mu\nu} c(x) \bar{d}(x)\gamma_\nu \gamma_5 u(x) \\ &\quad \left. - i\bar{c}(x)\sigma^{\mu\nu} \gamma_5 u(x) \bar{d}(x)\gamma_\nu c(x) + i\bar{c}(x)\gamma_\nu u(x) \bar{d}(x)\sigma^{\mu\nu} \gamma_5 c(x) \right\},\end{aligned}\tag{9}$$

while the constituents, such as $\bar{c}(x)i\gamma_5 c(x) \bar{d}(x)\gamma^\mu u(x)$, $\bar{c}(x)\gamma^\mu c(x) \bar{d}(x)i\gamma_5 u(x)$, etc, couple potentially to the meson-meson type scattering states or tetraquark molecular states.

However, we should be careful in performing the Fierz rearrangements, the rearrangements in the spinor space and color space are quite non-trivial, the scenarios of the diquark-antidiquark type tetraquark states and meson-meson type molecular states are quite different.

According to the arguments of Selem and Wilczek, a diquark-antidiquark type tetraquark can be plausibly described by two diquarks trapped in a double potential well, the two potential wells are separated apart by a barrier [37]. At long distances, the diquark and antidiquark serve as point color charges respectively, and attract each other strongly just like in the quark and antiquark bound states. However, when the two diquarks approach each other, the attractions between quark and antiquark in different diquarks decrease the bound energy of the diquarks and tend to destroy the diquarks. Those effects (beyond the naive one-gluon exchange force) increase when the distance between the diquark and antidiquark decreases, and a repulsive interaction between the diquark and antidiquark emerges, if large enough, it will lead to a barrier between the diquark and antidiquark [38]. The two potential wells which are separated apart by a barrier can give successful descriptions of the diquark-antidiquark type tetraquark states [38].

While in the dynamical picture of the tetraquark states, the large spatial separation between the diquark and antidiquark leads to small wave-function overlap between the quark-antiquark pair [39], the rearrangements in the spinor space and color space are highly suppressed.

In practical calculations, it is difficult to account for the non-local effects between the diquark and antidiquark pair in the four-quark currents $J_\mu(x)$ and $J_{\mu\nu}(x)$ directly, for example, the current $J_\mu^1(x)$ can be modified to

$$\begin{aligned}J_\mu^1(x, \epsilon) &= \frac{\varepsilon^{ijk} \varepsilon^{imn}}{\sqrt{2}} \left[u^{Tj}(x) C \gamma_5 c^k(x) \bar{d}^m(x + \epsilon) \gamma_\mu C \bar{c}^{Tn}(x + \epsilon) - u^{Tj}(x) C \gamma_\mu c^k(x) \bar{d}^m(x + \epsilon) \right. \\ &\quad \left. \gamma_5 C \bar{c}^{Tn}(x + \epsilon) \right],\end{aligned}\tag{10}$$

to account for the non-locality by adding a finite ϵ , however, it is very difficult to deal with the finite ϵ both at the hadron side and at the QCD side in a consistent way, we expend the current

$J_\mu^1(x, \epsilon)$ in terms of Taylor series of ϵ ,

$$J_\mu^1(x, \epsilon) = J_\mu^1(x, 0) + \frac{\partial J_\mu^1(x, \epsilon)}{\partial \epsilon^\alpha} \Big|_{\epsilon=0} \epsilon^\alpha + \frac{1}{2} \frac{\partial^2 J_\mu^1(x, \epsilon)}{\partial \epsilon^\alpha \partial \epsilon^\beta} \Big|_{\epsilon=0} \epsilon^\alpha \epsilon^\beta + \dots, \quad (11)$$

then expand the correlation function $\Pi_{\mu\nu}(p)$ also in terms of Taylor series of ϵ ,

$$\Pi_{\mu\nu}(p) = \Pi_{\mu\nu}(\mathcal{O}(\epsilon^0)) + \Pi_{\mu\nu}(\mathcal{O}(\epsilon^1)) + \Pi_{\mu\nu}(\mathcal{O}(\epsilon^2)) + \dots, \quad (12)$$

where the components $\Pi_{\mu\nu}(\mathcal{O}(\epsilon^i))$ with $i = 0, 1, 2, \dots$ stand for the contributions of the order $\mathcal{O}(\epsilon^i)$. In this article, we study the leading order contributions $J_\mu^1(x) = J_\mu^1(x, 0)$ and $\Pi_{\mu\nu}(p) = \Pi_{\mu\nu}(\mathcal{O}(\epsilon^0))$, the effects beyond the leading order frustrate the Fierz rearrangements of the diquark-antidiquark type currents into a series of color-singlet-color-singlet (meson-meson) type currents freely.

We can use the Feynman diagram drawn in Fig.1 to describe the lowest order contributions in the correlation functions for the diquark-antidiquark type four-quark currents, and use the Feynman diagrams drawn in Fig.2 to describe the corresponding lowest order contributions in the correlation functions for the color-singlet-color-singlet type four-quark currents. The Feynman diagram drawn in Fig.1 cannot be factorized into the two Feynman diagrams drawn in Fig.2 freely due to the barrier (or spatial separation) between the diquark and antidiquark [38, 39]. When a quark (antiquark) in the diquark (antidiquark) penetrates the barrier, the Feynman diagram drawn in Fig.1 is factorizable in color space. In this case, the non-factorizable diagrams start at the order $\mathcal{O}(\alpha_s^2)$ [40].

In Ref.[40], Lucha, Melikhov, and Sazdjian argue that the diquark-antidiquark type four-quark currents can be changed into the color-singlet-color-singlet (meson-meson) type currents through Fierz transformation, the Feynman diagrams which make contributions to the quark-gluon operators of the order $\mathcal{O}(\alpha_s^0)$ and $\mathcal{O}(\alpha_s)$ in accomplishing the operator product expansion are factorizable and are canceled out by the contributions of the two-meson scattering states at the phenomenological side, furthermore, the factorizable parts (in color space) of the Feynman diagrams of the order $\mathcal{O}(\alpha_s^2)$ are also canceled out by the contributions come from the two-meson scattering states (or more precisely, the free two-meson states), the relevant non-factorizable contributions start at the order $\mathcal{O}(\alpha_s^2)$. We do not agree with their viewpoint, as there exists a repulsive barrier [37, 38] or a large spatial separation [39], which are embodied in the non-local effects, to prevent performing the Fierz transformation freely, although at the present time we cannot take into account the non-local effects in the QCD sum rules, and have to take the leading order approximations $J_\mu^1(x) = J_\mu^1(x, 0)$ and $\Pi_{\mu\nu}(p) = \Pi_{\mu\nu}(\mathcal{O}(\epsilon^0))$. Our viewpoint is that the relevant contributions begin at the order $\mathcal{O}(\alpha_s^0)$, it is not necessary to perform or it is very difficult to perform the Fierz transformation to separate the factorizable and non-factorizable contributions in the color space, we should take into account both the factorizable and nonfactorizable Feynman diagrams for the diquark-antidiquark type currents.

When the quark or antiquark penetrates the barrier, we can perform the Fierz rearrangements, and study the effects of the scattering states. Now let us begin to explore the contributions of the meson-meson type scattering states (in other words, the two-meson loops) to the Green function $\Pi_{\mu\nu}(p)$ for the four-quark current $J_\mu^1(x)$ as a representative example,

$$\begin{aligned} \Pi_{\mu\nu}(p) &= -\frac{\widehat{\lambda}_Z^2}{p^2 - \widehat{M}_Z^2} \widetilde{g}_{\mu\nu}(p) - \frac{\widehat{\lambda}_Z}{p^2 - \widehat{M}_Z^2} \widetilde{g}_{\mu\alpha}(p) \Sigma_{DD^*}(p) \widetilde{g}^{\alpha\beta}(p) \widetilde{g}_{\beta\nu}(p) \frac{\widehat{\lambda}_Z}{p^2 - \widehat{M}_Z^2} \\ &\quad - \frac{\widehat{\lambda}_Z}{p^2 - \widehat{M}_Z^2} \widetilde{g}_{\mu\alpha}(p) \Sigma_{J/\psi\pi}(p) \widetilde{g}^{\alpha\beta}(p) \widetilde{g}_{\beta\nu}(p) \frac{\widehat{\lambda}_{X/Z}}{p^2 - \widehat{M}_Z^2} + \dots, \\ &= -\frac{\widehat{\lambda}_Z^2}{p^2 - \widehat{M}_Z^2 - \Sigma_{DD^*}(p) - \Sigma_{J/\psi\pi}(p) + \dots} \widetilde{g}_{\mu\nu}(p) + \dots, \end{aligned} \quad (13)$$

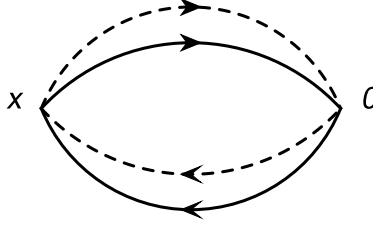


Figure 1: The Feynman diagram of the lowest order contributions for the diquark-antidiquark type currents, where the solid lines represent the light quarks and dashed lines represent the heavy quarks.

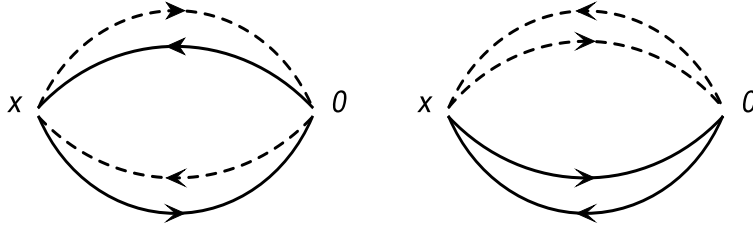


Figure 2: The Feynman diagrams of the lowest order contributions for the color-singlet-color-singlet type currents, where the solid lines represent the light quarks and dashed lines represent the heavy quarks.

where

$$\begin{aligned}\Sigma_{DD^*}(p) &= i \int \frac{d^4q}{(2\pi)^4} \frac{G_{ZDD^*}^2}{[q^2 - M_D^2][(p-q)^2 - M_{D^*}^2]}, \\ \Sigma_{J/\psi\pi}(p) &= i \int \frac{d^4q}{(2\pi)^4} \frac{G_{ZJ/\psi\pi}^2}{[q^2 - M_{J/\psi}^2][(p-q)^2 - M_\pi^2]},\end{aligned}\quad (14)$$

$\tilde{g}_{\mu\nu}(p) = -g_{\mu\nu} + \frac{p_\mu p_\nu}{p^2}$, the G_{ZDD^*} and $G_{ZJ/\psi\pi}$ are the hadronic coupling constants. We resort to the bare quantities $\hat{\lambda}_Z$ and \hat{M}_Z so as to absorb the divergent terms which appear in the integrals in calculating the self-energies $\Sigma_{DD^*}(p)$, $\Sigma_{J/\psi\pi}(p)$, etc. The self-energies after renormalization result in a finite energy-dependent width to modify the dispersion relation,

$$\Pi_{\mu\nu}(p) = -\frac{\lambda_Z^2}{p^2 - M_Z^2 + i\sqrt{p^2}\Gamma(p^2)}\tilde{g}_{\mu\nu}(p) + \dots, \quad (15)$$

the experimental value of the total decay width $\Gamma_{Z_c(3900)}(M_Z^2) = (46 \pm 10 \pm 20) \text{ MeV}$ [4] (or $(28.2 \pm 2.6) \text{ MeV}$ [9]), the zero width approximation in the spectral densities at the phenomenological side are approved reasonable [41]. In this paper, we neglect the contributions of the meson-meson type scattering states or the two-meson loops, the predictions are still robust.

We calculate all the Feynman diagrams in performing the operator product expansion to obtain the QCD spectral representation of the Green functions (or correlation functions) $\Pi_{\mu\nu}(p)$ and $\Pi_{\mu\nu\alpha\beta}(p)$. In analytical calculations, we take into account the vacuum condensates (by selecting the quark-gluon operators of the orders $\mathcal{O}(\alpha_s^k)$ with $k \leq 1$) up to dimension 10 consistently and factorize the higher dimensional condensates into the lower dimensional condensates by assuming vacuum saturation. After getting the analytical expressions of the Green functions at the quark-gluon level, we obtain the spectral representation via dispersion relation. Now we match the hadronic representation with the QCD representation of the Green functions (or correlation functions) $\Pi_Z(p^2)$ below the continuum threshold parameters s_0 and carry out the Borel transformation

in regard to $P^2 = -p^2$ to get the QCD sum rules:

$$\lambda_Z^2 \exp\left(-\frac{M_Z^2}{T^2}\right) = \int_{4m_c^2}^{s_0} ds \rho(s) \exp\left(-\frac{s}{T^2}\right), \quad (16)$$

$$\rho(s) = \rho_0(s) + \rho_3(s) + \rho_4(s) + \rho_5(s) + \rho_6(s) + \rho_7(s) + \rho_8(s) + \rho_{10}(s), \quad (17)$$

$\lambda_Z = \tilde{\lambda}_Z M_Z$, the T^2 is the Borel parameter, the subscripts i in the components of the QCD spectral densities $\rho_i(s)$ represent the dimensions of the vacuum condensates,

$$\begin{aligned} \rho_3(s) &\propto \langle \bar{q}q \rangle, \\ \rho_4(s) &\propto \left\langle \frac{\alpha_s GG}{\pi} \right\rangle, \\ \rho_5(s) &\propto \langle \bar{q}g_s \sigma Gq \rangle, \\ \rho_6(s) &\propto \langle \bar{q}q \rangle^2, 4\pi\alpha_s \langle \bar{q}q \rangle^2, \\ \rho_7(s) &\propto \langle \bar{q}q \rangle \left\langle \frac{\alpha_s GG}{\pi} \right\rangle, \\ \rho_8(s) &\propto \langle \bar{q}q \rangle \langle \bar{q}g_s \sigma Gq \rangle, \\ \rho_{10}(s) &\propto \langle \bar{q}g_s \sigma Gq \rangle^2, \langle \bar{q}q \rangle^2 \left\langle \frac{\alpha_s GG}{\pi} \right\rangle. \end{aligned} \quad (18)$$

We neglect the cumbersome analytical expressions of the spectral densities at the quark-gluon level in saving printed pages. We can refer to Ref.[20] for the technical details in calculating the Feynman diagrams. On the other hand, we can refer to Refs.[20, 23] for the explicit expressions of the spectral densities at the quark-gluon level for the axialvector current $J_\mu^1(x)$ and tensor current $J_{\mu\nu}(x)$. In this work, we recalculate those QCD spectral densities, and use the formula $t_{ij}^a t_{mn}^a = -\frac{1}{6}\delta_{ij}\delta_{mn} + \frac{1}{2}\delta_{jm}\delta_{in}$ with $t^a = \frac{\lambda^a}{2}$ to deal with the higher dimensional vacuum condensates, where the λ^a is the Gell-Mann matrix. This routine leads to slight but neglectful differences compared to the old calculations. For the currents $J_\mu^2(x)$ and $J_\mu^3(x)$, we neglect the tiny contributions of the $4\pi\alpha_s \langle \bar{q}q \rangle^2$, which originate from the operators like $\langle \bar{q}_j \gamma_\mu q_i g_s D_\nu G_{\alpha\beta}^a t_{mn}^a \rangle$.

We derive Eq.(16) in regard to $\tau = \frac{1}{T^2}$, then reach the QCD sum rules for the tetraquark masses by eliminating the pole residues λ_Z through a fraction,

$$M_Z^2 = -\frac{\int_{4m_c^2}^{s_0} ds \frac{d}{d\tau} \rho(s) e^{-\tau s}}{\int_{4m_c^2}^{s_0} ds \rho(s) e^{-\tau s}}. \quad (19)$$

Thereafter, we will refer the QCD sum rules in Eq.(16) and Eq.(19) as QCDSR I.

If we take into account the contributions of the first radially excited tetraquark states Z'_c in the hadronic representation, we can obtain the QCD sum rules,

$$\lambda_Z^2 \exp\left(-\frac{M_Z^2}{T^2}\right) + \lambda_{Z'}^2 \exp\left(-\frac{M_{Z'}^2}{T^2}\right) = \int_{4m_c^2}^{s'_0} ds \rho(s) \exp\left(-\frac{s}{T^2}\right), \quad (20)$$

where the s'_0 is continuum threshold parameter, then we introduce the notations $\tau = \frac{1}{T^2}$, $D^n = \left(-\frac{d}{d\tau}\right)^n$, and resort to the subscripts 1 and 2 to represent the ground state tetraquark state Z_c and the first radially excited tetraquark state Z'_c respectively for simplicity. We rewrite the QCD sum rules as

$$\lambda_1^2 \exp(-\tau M_1^2) + \lambda_2^2 \exp(-\tau M_2^2) = \Pi_{QCD}(\tau), \quad (21)$$

here we introduce the subscript QCD to represent the QCD representation. We derive the QCD sum rules in Eq.(21) in regard to τ to get

$$\lambda_1^2 M_1^2 \exp(-\tau M_1^2) + \lambda_2^2 M_2^2 \exp(-\tau M_2^2) = D\Pi_{QCD}(\tau). \quad (22)$$

From Eqs.(21)-(22), we obtain the QCD sum rules,

$$\lambda_i^2 \exp(-\tau M_i^2) = \frac{(D - M_j^2) \Pi_{QCD}(\tau)}{M_i^2 - M_j^2}, \quad (23)$$

where the indexes $i \neq j$. Let us derive the QCD sum rules in Eq.(23) in regard to τ to get

$$\begin{aligned} M_i^2 &= \frac{(D^2 - M_j^2 D) \Pi_{QCD}(\tau)}{(D - M_j^2) \Pi_{QCD}(\tau)}, \\ M_i^4 &= \frac{(D^3 - M_j^2 D^2) \Pi_{QCD}(\tau)}{(D - M_j^2) \Pi_{QCD}(\tau)}. \end{aligned} \quad (24)$$

The squared masses M_i^2 satisfy the equation,

$$M_i^4 - bM_i^2 + c = 0, \quad (25)$$

where

$$\begin{aligned} b &= \frac{D^3 \otimes D^0 - D^2 \otimes D}{D^2 \otimes D^0 - D \otimes D}, \\ c &= \frac{D^3 \otimes D - D^2 \otimes D^2}{D^2 \otimes D^0 - D \otimes D}, \\ D^j \otimes D^k &= D^j \Pi_{QCD}(\tau) D^k \Pi_{QCD}(\tau), \end{aligned} \quad (26)$$

the indexes $i = 1, 2$ and $j, k = 0, 1, 2, 3$. Finally we solve above equation analytically to obtain two solutions [30],

$$M_1^2 = \frac{b - \sqrt{b^2 - 4c}}{2}, \quad (27)$$

$$M_2^2 = \frac{b + \sqrt{b^2 - 4c}}{2}. \quad (28)$$

From now on, we will denote the QCD sum rules in Eq.(20) and Eqs.(27)-(28) as QCDSR II. In calculations, we observe that if we specify the energy scales of the spectral densities in the QCD representation, only one solution satisfies the energy scale formula $\mu = \sqrt{M_{X/Y/Z}^2 - (2M_c)^2}$ in the QCDSR II, we have to abandon the other solution. In this paper, we retain the mass M_2 ($M_{Z'}$) and discard the mass M_1 (M_Z).

3 Numerical results and discussions

We take the standard values or conventional values of the vacuum condensates $\langle \bar{q}q \rangle = -(0.24 \pm 0.01 \text{ GeV})^3$, $\langle \bar{q}g_s \sigma Gq \rangle = m_0^2 \langle \bar{q}q \rangle$, $m_0^2 = (0.8 \pm 0.1) \text{ GeV}^2$, $\langle \frac{\alpha_s GG}{\pi} \rangle = (0.33 \text{ GeV})^4$ at the typical energy scale $\mu = 1 \text{ GeV}$ [35, 36, 42], and take the modified minimal subtraction mass of the charm quark $m_c(m_c) = (1.275 \pm 0.025) \text{ GeV}$ from the Particle Data Group [9]. We should evolve the quark condensate, mixed quark condensate and modified minimal subtraction mass to a special energy scale to warrant the parameters in the QCD spectral densities having the same energy scale. Now

let us account for the energy-scale dependence of the input parameters at the quark-gluon level,

$$\begin{aligned}
\langle \bar{q}q \rangle(\mu) &= \langle \bar{q}q \rangle(1\text{GeV}) \left[\frac{\alpha_s(1\text{GeV})}{\alpha_s(\mu)} \right]^{\frac{12}{33-2n_f}}, \\
\langle \bar{q}g_s\sigma Gq \rangle(\mu) &= \langle \bar{q}g_s\sigma Gq \rangle(1\text{GeV}) \left[\frac{\alpha_s(1\text{GeV})}{\alpha_s(\mu)} \right]^{\frac{2}{33-2n_f}}, \\
m_c(\mu) &= m_c(m_c) \left[\frac{\alpha_s(\mu)}{\alpha_s(m_c)} \right]^{\frac{12}{33-2n_f}}, \\
\alpha_s(\mu) &= \frac{1}{b_0 t} \left[1 - \frac{b_1 \log t}{b_0^2 t} + \frac{b_1^2 (\log^2 t - \log t - 1) + b_0 b_2}{b_0^4 t^2} \right], \tag{29}
\end{aligned}$$

where $t = \log \frac{\mu^2}{\Lambda^2}$, $b_0 = \frac{33-2n_f}{12\pi}$, $b_1 = \frac{153-19n_f}{24\pi^2}$, $b_2 = \frac{2857 - \frac{5033}{9}n_f + \frac{325}{27}n_f^2}{128\pi^3}$, with the values $\Lambda = 210$ MeV, 292 MeV and 332 MeV for the quark flavors $n_f = 5, 4$ and 3, respectively [9, 43]. As we explore the hidden-charm tetraquark states, we choose the flavor $n_f = 4$ and search for the best energy scales μ .

The Okubo-Zweig-Iizuka supper-allowed decays

$$\begin{aligned}
Z_c &\rightarrow J/\psi\pi, \\
Z'_c &\rightarrow \psi'\pi \\
Z''_c &\rightarrow \psi''\pi, \tag{30}
\end{aligned}$$

are expected to take place easily. The energy gaps maybe have the relations $M_{Z'} - M_Z = m_{\psi'} - m_{J/\psi}$ and $M_{Z''} - M_{Z'} = m_{\psi''} - m_{\psi'}$. The charmonium masses are $m_{J/\psi} = 3.0969$ GeV, $m_{\psi'} = 3.686097$ GeV and $m_{\psi''} = 4.039$ GeV from the Particle Data Group [9], $m_{\psi'} - m_{J/\psi} = 0.59$ GeV, $m_{\psi''} - m_{J/\psi} = 0.94$ GeV, we can choose the continuum threshold parameters to be $\sqrt{s_0} = M_Z + 0.59$ GeV and $\sqrt{s'_0} = M_Z + 0.95$ GeV tentatively and vary the continuum threshold parameters and Borel parameters to satisfy the following four criteria:

1. The ground state tetraquark state or single-pole term makes dominant contribution at the hadron side;
2. The operator product expansion is convergent below the continuum thresholds, and the higher dimensional vacuum condensates make minor contribution;
3. The Borel platforms appear in both the lineshapes of the tetraquark masses and pole residues with variations of the Borel parameters;
4. The masses of the tetraquark states satisfy the energy-scale formula.

After trial and error, we reach the feasible continuum threshold parameters and Borel windows, we also acquire the best energy scales of the spectral densities at the quark-gluon level and the contributions of the ground state tetraquark states for the QCDSR I, see Table 1. In general, for the continuum threshold parameters s_0 , we can take any values satisfy the relation $M_{gr} < \sqrt{s_0} \leq M_{gr} + \Delta$, where the subscript *gr* denotes the ground states, as there exists an energy gap Δ between the ground state and the first radial excited state. For the conventional S-wave quark-antiquark mesons, the energy gaps Δ vary from $m_{m_{K^*(1410)}} - m_{K^*(892)} = 522$ MeV to $m_{\pi(1300)} - m_{\pi} = 1160$ MeV, i.e. $\Delta = 522 \sim 1160$ MeV [9]. In the QCD sum rules for the conventional quark-antiquark mesons, we usually choose the values $\sqrt{s_0} = M_{gr} + (0.4 \sim 0.7)$ GeV [42]. In Table 1, the continuum threshold parameters s_0 satisfy the relation $\sqrt{s_0} = M_{Z_c} + (0.4 \sim 0.6)$ GeV or $M_{Z_c} + (0.5 \sim 0.7)$ GeV, it is reasonable, as the values $\exp(-s_{max}^0/T_{max}^2) = (1 \sim 2)\%$, where the subscript *max* denotes the maximum values, the contributions of the Z'_c are greatly suppressed if there are any. In Table 1, we write the continuum threshold parameters as $s_0 = 21.0 \pm 1.0$ GeV² rather than as $s_0 = (4.58 \pm 0.11 \text{ GeV})^2$ for the $[uc]_A[\bar{d}\bar{c}]_A - [uc]_A[\bar{d}\bar{c}]_A$ and $[uc]_A[\bar{d}\bar{c}]_A$ tetraquark states to retain the same form as in our previous work [23]. In Ref.[23], we study the axialvector $[uc]_A[\bar{d}\bar{c}]_A$ tetraquark state and choose the continuum threshold parameters as $s_0 = 21.0 \pm 1.0$ GeV².

Again we obtain the corresponding parameters for the QCDSR II using trial and error, see Table 2. In this paper, we employ the energy scale formula $\mu = \sqrt{M_{X/Y/Z}^2 - (2M_c)^2}$ with the effective charm quark mass (or constituent charm quark mass) M_c to restrain the tetraquark masses and the energy scales of the spectral densities [31]. The energy scale formula can enhance the contributions of the ground state tetraquark states remarkably at the hadron representation and improve the convergent behaviors of the operator product expansion remarkably at the QCD representation by augmenting the contributions of the lower dimensional vacuum condensates, and is feasible for the hidden-charm tetraquark states and hidden-charm pentaquark states [44].

From Table 1 and Table 2, we can see that the contributions of the single-pole terms (the ground state tetraquark states) are about (40 – 60)% for the QCDSR I, the contributions of the two-pole terms (the ground state tetraquark states plus the first radially excited tetraquark states) are about (70 – 80)% for the QCDSR II, which satisfy the pole dominance criterion very well. In the QCDSR II, the contributions of the ground state tetraquark states are about (30 – 45)%, which are much less than the corresponding ground state tetraquark contributions in the QCDSR I, for the ground state tetraquark masses and pole residues, we prefer the predictions from the QCDSR I. In numerical calculations, we find that the contributions of the vacuum condensates of dimension 10 (the largest dimension) are of percent level at the Borel windows for both the QCDSR I and QCDSR II, the minor contributions warrant good convergent behaviors of the operator product expansion.

Now let us take into account all the uncertainties of input parameters, and reach the numerical values of the masses and pole residues of the ground state tetraquark states Z_c and the first radially excited tetraquark states Z'_c , which are shown in Table 3 and Table 4. From those Tables, we can see that the ground state tetraquark masses from the QCDSR I and the radially excited tetraquark masses from the QCDSR II satisfy the energy scale formula $\mu = \sqrt{M_{X/Y/Z}^2 - (2M_c)^2}$, where the updated value of the effective charm quark mass (or constituent charm quark mass) $M_c = 1.82$ GeV is adopted [23]. In Table 4, we also present the central values of the ground state tetraquark masses and pole residues extracted from the QCDSR II at the ideal energy scales which are shown in Table 1. We examine Table 4 and observe that the ground state tetraquark masses cannot satisfy the energy scale formula, so we will discard those values. This is the shortcoming of the QCDSR II.

In Fig.3, we plot the ground state tetraquark masses from the QCDSR I and the first radially excited tetraquark masses from the QCDSR II in regard to variations of the Borel parameters in much larger regions than the Borel windows, which are shown in Table 1 and Table 2. From the Fig.3, we find that there indeed appear very flat platforms in the Borel windows for the $[uc]_S[\bar{d}\bar{c}]_A - [uc]_A[\bar{d}\bar{c}]_S$ type, $[uc]_{\bar{A}}[\bar{d}\bar{c}]_A - [uc]_A[\bar{d}\bar{c}]_{\bar{A}}$ type and $[uc]_A[\bar{d}\bar{c}]_A$ type axialvector tetraquark states. For the $[uc]_{\bar{V}}[\bar{d}\bar{c}]_V + [uc]_V[\bar{d}\bar{c}]_{\bar{V}}$ type tetraquark state, we only plot the ground state tetraquark mass, as the ground state tetraquark mass is large enough. From the Fig.3, we also find that the platform in the Borel window is not flat enough, at the region $T^2 < 3.6$ GeV², the mass increases quickly and monotonously along with the increase of the value of Borel parameter, the platform appears approximately only at the region $T^2 > 3.6$ GeV².

The predicted mass $M_Z = 3.90 \pm 0.08$ GeV for the ground state tetraquark state $[uc]_S[\bar{d}\bar{c}]_A - [uc]_A[\bar{d}\bar{c}]_S$ exhibits very good agreement with the experimental value $M_{Z(3900)} = (3899.0 \pm 3.6 \pm 4.9)$ MeV from the BESIII collaboration [4], which is in favor of assigning the $Z_c(3900)$ to be the ground state tetraquark state $[uc]_S[\bar{d}\bar{c}]_A - [uc]_A[\bar{d}\bar{c}]_S$ with the quantum numbers $J^{PC} = 1^{+-}$ [20]. In Ref.[45], we study the non-leptonic decays $Z_c^+(3900) \rightarrow J/\psi\pi^+, \eta_c\rho^+, D^+\bar{D}^{*0}, \bar{D}^0 D^{*+}$ with the three-point QCD sum rules. In analytical calculations, we take into account both the factorizable and nonfactorizable Feynman diagrams, match the hadronic representation with the QCD representation according to solid quark-hadron duality, and get the total decay width $\Gamma_{Z_c} = 54.2 \pm 29.8$ MeV, which agrees with the experimental value $(46 \pm 10 \pm 20)$ MeV very good considering the uncertainties [4].

The predicted mass $M_Z = 4.47 \pm 0.09$ GeV for the first radially excited tetraquark state $[uc]_S[\bar{d}\bar{c}]_A - [uc]_A[\bar{d}\bar{c}]_S$ exhibits very good agreement with the experimental value $M_{Z(4430)} =$

($4475 \pm 7_{-25}^{+15}$) MeV from the LHCb collaboration [10], which is in favor of assigning the $Z_c(4430)$ to be the first radially excited tetraquark state $[uc]_S[\bar{d}\bar{c}]_A - [uc]_A[\bar{d}\bar{c}]_S$ with the quantum numbers $J^{PC} = 1^{+-}$. We can investigate its non-leptonic decays with the three-point QCD sum rules to make more reasonable assignment.

The predicted mass $M_Z = 4.01 \pm 0.09$ GeV for the ground state tetraquark state $[uc]_{\bar{A}}[\bar{d}\bar{c}]_A - [uc]_A[\bar{d}\bar{c}]_{\bar{A}}$ and $M_Z = 4.00 \pm 0.09$ GeV for the ground state tetraquark state $[uc]_A[\bar{d}\bar{c}]_A$ both exhibit very good agreement with the experimental values $M_{Z(4020/4025)} = (4026.3 \pm 2.6 \pm 3.7)$ MeV [7] and $(4022.9 \pm 0.8 \pm 2.7)$ MeV [8] from the BESIII collaboration. There are two axialvector tetraquark state candidates with the quantum numbers $J^{PC} = 1^{+-}$ for the $Z_c(4020)$. Again the two-body strong decays should be studied to make the assignment more reasonably.

The predicted mass $M_Z = 4.60 \pm 0.09$ GeV for the first radially excited tetraquark state $[uc]_{\bar{A}}[\bar{d}\bar{c}]_A - [uc]_A[\bar{d}\bar{c}]_{\bar{A}}$ and $M_Z = 4.58 \pm 0.09$ GeV for the first radially excited tetraquark state $[uc]_A[\bar{d}\bar{c}]_A$ both exhibit very good agreement with the experimental value $M_{Z(4600)} = 4600$ MeV from the LHCb collaboration [1]. On the other hand, the predicted mass $M_Z = 4.66 \pm 0.10$ GeV for the ground state tetraquark state $[uc]_{\bar{V}}[\bar{d}\bar{c}]_V + [uc]_V[\bar{d}\bar{c}]_{\bar{V}}$ is also compatible with the experimental data $M_{Z(4600)} = 4600$ MeV from the LHCb collaboration [1]. Furthermore, the decay $Z_c(4600) \rightarrow J/\psi\pi$ can take place more easily for the ground state tetraquark state, which is in very good agreement with the observation of the $Z_c(4600)$ in the $J/\psi\pi$ invariant mass spectrum [1]. In summary, there are three axialvector tetraquark state candidates with $J^{PC} = 1^{+-}$ for the $Z_c(4600)$, we still need more theoretical and experimental works to identify the $Z_c(4600)$ unambiguously.

In Ref.[2], we identify the $Z_c(4600)$ as the $[dc]_P[\bar{u}\bar{c}]_A - [dc]_A[\bar{u}\bar{c}]_P$ type vector tetraquark state tentatively according to the predicted mass $M_Z = (4.59 \pm 0.08)$ GeV from the QCD sum rules [46], and explore its non-leptonic decays $Z_c(4600) \rightarrow J/\psi\pi, \eta_c\rho, J/\psi a_0, \chi_{c0}\rho, D^*\bar{D}^*, D\bar{D}, D^*\bar{D}$ and $D\bar{D}^*$ with the QCD sum rules by matching the hadronic representation with the QCD representation with solid quark-hadron duality. The large partial decay width $\Gamma(Z_c^-(4600) \rightarrow J/\psi\pi^-) = 41.4_{-14.9}^{+20.5}$ MeV exhibits very good agreement with the observation of the $Z_c(4600)$ in the $J/\psi\pi^-$ invariant mass spectrum.

In Table 3, we also present the diquark spin S_{uc} , antidiquark spin $S_{\bar{d}\bar{c}}$ and total spin S of the hidden-charm tetraquark states. We examine the Table and find that the $[uc]_{\bar{A}}[\bar{d}\bar{c}]_A - [uc]_A[\bar{d}\bar{c}]_{\bar{A}}$ and $[uc]_A[\bar{d}\bar{c}]_A$ tetraquark states (which have the tetraquark structures $|1^+, 1; 1\rangle - |1, 1^+; 1\rangle$ and $|1, 1; 1\rangle$, respectively) have slightly larger masses than the $[uc]_S[\bar{d}\bar{c}]_A - [uc]_A[\bar{d}\bar{c}]_S$ tetraquark state (which has the structure $|0, 1; 1\rangle - |1, 0; 1\rangle$). It is reasonable, as the most favored diquark configurations or quark-quark correlations from the attractive interaction in the color-antitriplet (color-triplet) channel induced by one-gluon exchange are the scalar diquark (antidiquark) states. In previous works, the scalar, pseudoscalar, vector and axialvector diquarks states have been investigated with the QCD sum rules, the scalar and axialvector heavy diquark states in the color-antitriplet have almost degenerate masses or have almost the same typical quark-quark correlation lengths, the mass gaps between the scalar and axialvector heavy diquark states are very small or tiny [33]. Furthermore, it agrees with the predictions of the simple constituent diquark-antidiquark model [27].

The vector (or P-wave) diquark states $[uc]_V$ and $[uc]_{\bar{V}}$ are expected to have larger masses than the axialvector (or S-wave) diquark states $[uc]_A$ and $[uc]_{\bar{A}}$, as there exists a relative P-wave between the light quark and heavy quark. In the case of the traditional $c\bar{u}$ charmed mesons, the energy exciting a P-wave costs about 458 MeV from the Particle Data Group [9],

$$\frac{5m_{D_2^*} + 3m_{D_1} + m_{D_0^*}}{9} - \frac{3m_{D^*} + m_D}{4} = 458 \text{ MeV}. \quad (31)$$

If the energy exciting a P-wave in the qc diquark systems also costs about 458 MeV, the $[uc]_{\bar{V}}[\bar{d}\bar{c}]_V + [uc]_V[\bar{d}\bar{c}]_{\bar{V}}$ tetraquark state has the largest ground state mass, which is even larger than the masses of the first radially excited states of the hidden-charm tetraquark states $[uc]_{\bar{A}}[\bar{d}\bar{c}]_A - [uc]_A[\bar{d}\bar{c}]_{\bar{A}}$ and $[uc]_A[\bar{d}\bar{c}]_A$ with the quantum numbers $J^{PC} = 1^{+-}$, as exciting two P-waves costs about 0.9 GeV,

Z_c	$T^2(\text{GeV}^2)$	s_0	$\mu(\text{GeV})$	pole
$[uc]_S[\bar{d}\bar{c}]_A - [uc]_A[\bar{d}\bar{c}]_S$	2.7 – 3.1	$(4.4 \pm 0.1 \text{ GeV})^2$	1.4	(40 – 63)%
$[uc]_{\bar{A}}[\bar{d}\bar{c}]_A - [uc]_A[\bar{d}\bar{c}]_{\bar{A}}$	3.2 – 3.6	$21.0 \pm 1.0 \text{ GeV}^2$	1.7	(40 – 60)%
$[uc]_{\bar{V}}[\bar{d}\bar{c}]_V + [uc]_V[\bar{d}\bar{c}]_{\bar{V}}$	3.7 – 4.1	$(5.25 \pm 0.10 \text{ GeV})^2$	2.9	(41 – 60)%
$[uc]_A[\bar{d}\bar{c}]_A$	3.2 – 3.6	$21.0 \pm 1.0 \text{ GeV}^2$	1.7	(41 – 61)%

Table 1: The Borel parameters, continuum threshold parameters, energy scales of the QCD spectral densities and pole contributions for the QCDSR I.

$Z_c + Z'_c$	$T^2(\text{GeV}^2)$	s_0	$\mu(\text{GeV})$	pole (Z_c)
$[uc]_S[\bar{d}\bar{c}]_A - [uc]_A[\bar{d}\bar{c}]_S$	2.7 – 3.1	$(4.85 \pm 0.10 \text{ GeV})^2$	2.6	(72 – 88)% ((35 – 52)%)
$[uc]_{\bar{A}}[\bar{d}\bar{c}]_A - [uc]_A[\bar{d}\bar{c}]_{\bar{A}}$	3.2 – 3.6	$(4.95 \pm 0.10 \text{ GeV})^2$	2.8	(64 – 80)% ((30 – 44)%)
$[uc]_A[\bar{d}\bar{c}]_A$	3.2 – 3.6	$(4.95 \pm 0.10 \text{ GeV})^2$	2.8	(64 – 81)% ((29 – 43)%)

Table 2: The Borel parameters, continuum threshold parameters, energy scales of the QCD spectral densities and pole contributions for the QCDSR II.

which is larger than the energy gap 0.6 GeV between the ground state hidden-charm tetraquark state and the first radial excitation of the hidden-charm tetraquark states.

4 Conclusion

In this paper, we investigate the ground states and the first radially excited states of the $[uc]_S[\bar{d}\bar{c}]_A - [uc]_A[\bar{d}\bar{c}]_S$ type, $[uc]_{\bar{A}}[\bar{d}\bar{c}]_A - [uc]_A[\bar{d}\bar{c}]_{\bar{A}}$ type and $[uc]_A[\bar{d}\bar{c}]_A$ type tetraquark states and the ground state $[uc]_{\bar{V}}[\bar{d}\bar{c}]_V + [uc]_V[\bar{d}\bar{c}]_{\bar{V}}$ type tetraquark state with the quantum numbers $J^{PC} = 1^{+-}$ via the QCD sum rules in a systematic way. The predicted tetraquark masses are in favor of assigning the $Z_c(3900)$ and $Z_c(4430)$ as the ground state and the first radially excited state of the $[uc]_S[\bar{d}\bar{c}]_A - [uc]_A[\bar{d}\bar{c}]_S$ type axialvector tetraquark states respectively; assigning the $Z_c(4020)$ as the ground state $[uc]_{\bar{A}}[\bar{d}\bar{c}]_A - [uc]_A[\bar{d}\bar{c}]_{\bar{A}}$ type axialvector tetraquark state or $[uc]_A[\bar{d}\bar{c}]_A$ type axialvector tetraquark state; assigning the $Z_c(4600)$ as the first radially excited $[uc]_{\bar{A}}[\bar{d}\bar{c}]_A - [uc]_A[\bar{d}\bar{c}]_{\bar{A}}$ type axialvector tetraquark state or $[uc]_A[\bar{d}\bar{c}]_A$ type axialvector tetraquark state, or the ground state $[uc]_{\bar{V}}[\bar{d}\bar{c}]_V + [uc]_V[\bar{d}\bar{c}]_{\bar{V}}$ type axialvector tetraquark state. We still need more experimental and theoretical works to identify the $Z_c(4600)$ unambiguously.

Z_c	$ S_{uc}, S_{\bar{d}\bar{c}}; S\rangle$	$M_Z(\text{GeV})$	$\lambda_Z(\text{GeV}^5)$
$[uc]_S[\bar{d}\bar{c}]_A - [uc]_A[\bar{d}\bar{c}]_S$	$ 0, 1; 1\rangle - 1, 0; 1\rangle$	3.90 ± 0.08	$(2.09 \pm 0.33) \times 10^{-2}$
$[uc]_{\bar{A}}[\bar{d}\bar{c}]_A - [uc]_A[\bar{d}\bar{c}]_{\bar{A}}$	$ 1^+, 1; 1\rangle - 1, 1^+; 1\rangle$	4.01 ± 0.09	$(5.96 \pm 0.94) \times 10^{-2}$
$[uc]_{\bar{V}}[\bar{d}\bar{c}]_V + [uc]_V[\bar{d}\bar{c}]_{\bar{V}}$	$ 1^-, 1; 1\rangle + 1, 1^-; 1\rangle$	4.66 ± 0.10	$(1.18 \pm 0.22) \times 10^{-1}$
$[uc]_A[\bar{d}\bar{c}]_A$	$ 1, 1; 1\rangle$	4.00 ± 0.09	$(2.91 \pm 0.46) \times 10^{-2}$

Table 3: The masses and pole residues of the ground state tetraquark states Z_c from the QCDSR I, where the superscripts \pm represent the positive parity and negative parity constituents of the tensor diquark states, respectively.

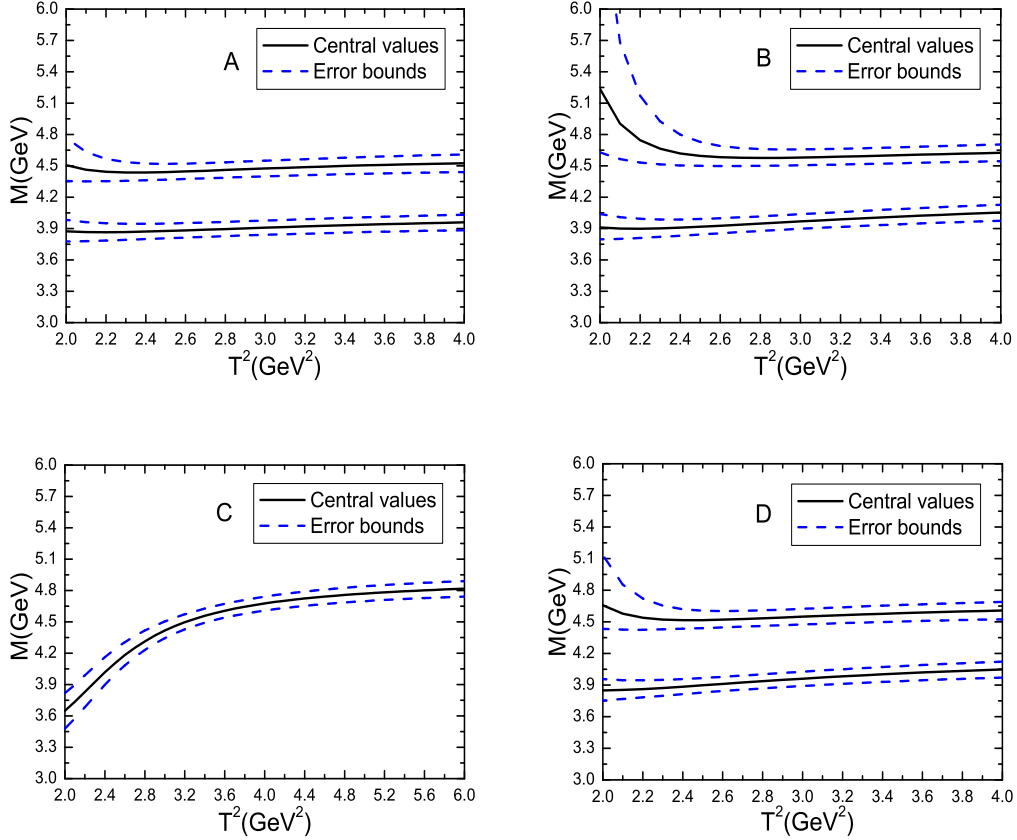


Figure 3: The masses with variations of the Borel parameters T^2 for the axialvector hidden-charm tetraquark states, the A , B , C and D represent the $[uc]_S[\bar{d}\bar{c}]_A - [uc]_A[\bar{d}\bar{c}]_S$, $[uc]_{\bar{A}}[\bar{d}\bar{c}]_A - [uc]_A[\bar{d}\bar{c}]_{\bar{A}}$, $[uc]_{\bar{V}}[\bar{d}\bar{c}]_V + [uc]_V[\bar{d}\bar{c}]_{\bar{V}}$ and $[uc]_A[\bar{d}\bar{c}]_A$ tetraquark states, respectively.

$Z_c + Z'_c$	$M_Z(\text{GeV})$	$\lambda_Z(\text{GeV}^3)$	$M_{Z'}(\text{GeV})$	$\lambda_{Z'}(\text{GeV}^3)$
$[uc]_S[\bar{d}\bar{c}]_A - [uc]_A[\bar{d}\bar{c}]_S$	3.81	1.77×10^{-2}	4.47 ± 0.09	$(6.02 \pm 0.80) \times 10^{-2}$
$[uc]_{\bar{A}}[\bar{d}\bar{c}]_A - [uc]_A[\bar{d}\bar{c}]_{\bar{A}}$	3.78	3.94×10^{-2}	4.60 ± 0.09	$(1.35 \pm 0.18) \times 10^{-1}$
$[uc]_A[\bar{d}\bar{c}]_A$	3.73	1.76×10^{-2}	4.58 ± 0.09	$(6.55 \pm 0.85) \times 10^{-2}$

Table 4: The masses and pole residues of the ground state tetraquark states Z_c and the first radially excited tetraquark states Z'_c from the QCDSR II.

Acknowledgements

This work is supported by National Natural Science Foundation, Grant Number 11775079.

References

- [1] R. Aaij et al, Phys. Rev. Lett. **122** (2019) 152002.
- [2] Z. G. Wang, Int. J. Mod. Phys. **A34** (2019) 1950110.
- [3] H. X. Chen and W. Chen, Phys. Rev. **D99** (2019) 074022.
- [4] M. Ablikim et al, Phys. Rev. Lett. **110** (2013) 252001.
- [5] Z. Q. Liu et al, Phys. Rev. Lett. **110** (2013) 252002.
- [6] T. Xiao, S. Dobbs, A. Tomaradze and K. K. Seth, Phys. Lett. **B727** (2013) 366.
- [7] M. Ablikim et al, Phys. Rev. Lett. **112** (2014) 132001.
- [8] M. Ablikim et al, Phys. Rev. Lett. **111** (2013) 242001.
- [9] M. Tanabashi et al, Phys. Rev. **D98** (2018) 030001.
- [10] R. Aaij et al, Phys. Rev. Lett. **112** (2014) 222002.
- [11] M. Ablikim et al, Phys. Rev. Lett. **119** (2017) 072001.
- [12] Q. Wang, C. Hanhart and Q. Zhao, Phys. Rev. Lett. **111** (2013) 132003.
- [13] F. K. Guo, C. Hidalgo-Duque, J. Nieves and M. P. Valderrama, Phys. Rev. **D88** (2013) 054007.
- [14] C. Y. Cui, Y. L. Liu, W. B. Chen and M. Q. Huang, J. Phys. **G41** (2014) 075003; J. R. Zhang, Phys. Rev. **D87** (2013) 116004.
- [15] Z. G. Wang and T. Huang, Eur. Phys. J. **C74** (2014) 2891; Z. G. Wang, Eur. Phys. J. **C74** (2014) 2963.
- [16] H. W. Ke, Z. T. Wei and X. Q. Li, Eur. Phys. J. **C73** (2013) 2561.
- [17] J. He, X. Liu, Z. F. Sun and S. L. Zhu, Eur. Phys. J. **C73** (2013) 2635.
- [18] Y. B. Dong, A. Faessler, T. Gutsche and V. E. Lyubovitskij, Phys. Rev. **D88** (2013) 014030.
- [19] L. Maiani, V. Riquer, R. Faccini, F. Piccinini, A. Pilloni and A. D. Polosa, Phys. Rev. **D87** (2013) 111102.
- [20] Z. G. Wang and T. Huang, Phys. Rev. **D89** (2014) 054019.
- [21] C. F. Qiao and L. Tang, Eur. Phys. J. **C74** (2014) 3122; C. F. Qiao and L. Tang, Eur. Phys. J. **C74** (2014) 2810.
- [22] Z. G. Wang, Commun. Theor. Phys. **63** (2015) 466.
- [23] Z. G. Wang, Eur. Phys. J. **C76** (2016) 387.
- [24] C. Deng, J. Ping and F. Wang, Phys. Rev. **D90** (2014) 054009.
- [25] X. H. Liu and G. Li, Phys. Rev. **D88** (2013) 014013.

- [26] D. Y. Chen, X. Liu and T. Matsuki, Phys. Rev. **D88** (2013) 036008; E. S. Swanson, Phys. Rev. **D91** (2015) 034009.
- [27] L. Maiani, F. Piccinini, A. D. Polosa and V. Riquer, Phys. Rev. **D89** (2014) 114010.
- [28] M. Nielsen and F. S. Navarra, Mod. Phys. Lett. **A29** (2014) 1430005.
- [29] Z. G. Wang, Commun. Theor. Phys. **63** (2015) 325.
- [30] M. S. Maior de Sousa and R. Rodrigues da Silva, Braz. J. Phys. **46** (2016) 730.
- [31] Z. G. Wang, Eur. Phys. J. **C74** (2014) 2874; Z. G. Wang and T. Huang, Nucl. Phys. **A930** (2014) 63.
- [32] S. S. Agaev, K. Azizi and H. Sundu, Phys. Rev. **D96** (2017) 034026.
- [33] Z. G. Wang, Eur. Phys. J. **C71** (2011) 1524; R. T. Kleiv, T. G. Steele and A. Zhang, Phys. Rev. **D87** (2013) 125018.
- [34] Z. G. Wang and J. X. Zhang, Eur. Phys. J. **C76** (2016) 650; Z. G. Wang and Z. Y. Di, Eur. Phys. J. **C79** (2019) 72.
- [35] M. A. Shifman, A. I. Vainshtein and V. I. Zakharov, Nucl. Phys. **B147** (1979) 385; Nucl. Phys. **B147** (1979) 448.
- [36] L. J. Reinders, H. Rubinstein and S. Yazaki, Phys. Rept. **127** (1985) 1.
- [37] A. Selem and F. Wilczek, hep-ph/0602128.
- [38] L. Maiani, A. D. Polosa and V. Riquer, Phys. Lett. **B778** (2018) 247.
- [39] S. J. Brodsky, D. S. Hwang and R. F. Lebed, Phys. Rev. Lett. **113** (2014) 112001.
- [40] W. Lucha, D. Melikhov and H. Sazdjian, Phys. Rev. **D100** (2019) 014010.
- [41] Z. G. Wang, Int. J. Mod. Phys. **A30** (2015) 1550168.
- [42] P. Colangelo and A. Khodjamirian, hep-ph/0010175.
- [43] S. Narison and R. Tarrach, Phys. Lett. **125 B** (1983) 217.
- [44] Z. G. Wang, Eur. Phys. J. **C76** (2016) 70; Z. G. Wang and T. Huang, Eur. Phys. J. **C76** (2016) 43.
- [45] Z. G. Wang and J. X. Zhang, Eur. Phys. J. **C78** (2018) 14.
- [46] Z. G. Wang, Eur. Phys. J. **C78** (2018) 518.